

Automatic Method for Avian Red Blood Cell and Heterophil Counting Using Iterative
Thresholding



A Thesis Submitted in Partial Fulfillment of the Requirements
for the Degree of Master of Engineering in Electrical Engineering

Department of Electrical Engineering

FACULTY OF ENGINEERING

Chulalongkorn University

Academic Year 2019

Copyright of Chulalongkorn University



จุฬาลงกรณ์มหาวิทยาลัย
CHULALONGKORN UNIVERSITY

วิธีตัดโน้มนิตสำหรับนับเม็ดเลือดแดงและเฮโมโกลบินของสัตว์ปีกโดยใช้การขีดแบ่งแบบวนซ้ำ



วิทยานิพนธ์นี้เป็นส่วนหนึ่งของการศึกษาตามหลักสูตรปริญญาวิศวกรรมศาสตรมหาบัณฑิต

สาขาวิชาวิศวกรรมไฟฟ้า ภาควิชาวิศวกรรมไฟฟ้า

คณะวิศวกรรมศาสตร์ จุฬาลงกรณ์มหาวิทยาลัย

ปีการศึกษา 2562

ลิขสิทธิ์ของจุฬาลงกรณ์มหาวิทยาลัย

Thesis Title Automatic Method for Avian Red Blood Cell and
Heterophil Counting Using Iterative Thresholding

By Mr. Tanapat Autaiem

Field of Study Electrical Engineering

Thesis Advisor Associate Professor SUPATANA AUETHAVEKIAT, Ph.D.

Thesis Co Advisor Vera Sa-ing, Ph.D.

Accepted by the FACULTY OF ENGINEERING, Chulalongkorn University in
Partial Fulfillment of the Requirement for the Master of Engineering

..... Dean of the FACULTY OF
ENGINEERING
(Professor SUPOT TEACHAVORASINSKUN, D.Eng.)

THESIS COMMITTEE

..... Chairman
(Associate Professor NISACHON TANGSANGIUMVISAI,
Ph.D.)

..... Thesis Advisor
(Associate Professor SUPATANA AUETHAVEKIAT, Ph.D.)

..... Thesis Co-Advisor
(Vera Sa-ing, Ph.D.)

..... External Examiner
(Noppadol Prasertsincharoen, Ph.D.)

ธนพัฒน์ อรรถเอี่ยม : วิธีอัตโนมัติสำหรับนับเม็ดเลือดแดงและเฮเทอโรฟิลของสัตว์ปีก โดยใช้การขีดแบ่งแบบวนซ้ำ. (Automatic Method for Avian Red Blood Cell and Heterophil Counting Using Iterative Thresholding) อ.ที่ปรึกษาหลัก : รศ. ดร.สุพัฒนา เอื้อทวิเกียรติ, อ.ที่ปรึกษาร่วม : ดร.วีระ สอึ้ง

ประเทศไทยเป็นหนึ่งในผู้ส่งออกไก่เนื้ออันดับต้น ๆ ของโลก จึงจำเป็นต้องทำการตรวจนับเม็ดเลือดไก่เพื่อควบคุมคุณภาพ เครื่องมือสำหรับนับเม็ดเลือดสัตว์เลี้ยงลูกด้วยนมนี้ไม่สามารถนำมาใช้กับสัตว์ปีกได้เนื่องจากลักษณะเม็ดเลือดที่แตกต่างกัน เพื่อที่จะทดแทนการนับด้วยมือ วิทยานิพนธ์นี้จึงได้นำเสนอวิธีการนับอัตโนมัติสำหรับเม็ดเลือดแดงและเฮเทอโรฟิล ซึ่งเป็นเม็ดเลือดขาวสัตว์ปีกชนิดที่พบได้มากที่สุด การตรวจพบเม็ดเลือดแดงสัตว์ปีกนั้นมีความยากอยู่ที่ รูปทรงเซลล์วงรี และมีนิวเคลียสอยู่ภายใน เซลล์ที่มีการทับซ้อนกัน และความหลากหลายของสีย้อมรูปสไลด์ วิธีการขีดแบ่งหลายระดับของไอซีได้ถูกนำมาใช้เพื่อดึงนิวเคลียสของเซลล์โดยตรงไม่โดยเกี่ยงสีย้อม จากนั้นจึงทำการวนซ้ำเพื่อแยกนิวเคลียสที่ติดกันโดยการลดค่าขีด ส่วนของการตรวจพบเฮเทอโรฟิลนั้น ทำโดยการลบเม็ดเลือดแดงที่ตรวจพบได้ออกก่อน แล้วตามด้วยการใช้ข้อมูลขอบเพื่อดึงพื้นที่เซลล์ จากนั้นจึงใช้กฎที่สร้างโดยสถิติเพื่อแยกเม็ดเลือดขาวออกมา ผลการทดลองแสดงให้เห็นว่า ค่าความผิดพลาดการนับเม็ดเลือดแดงสำหรับรูปสไลด์ 4 ใน 5 แบบ ได้ 8.8%

จุฬาลงกรณ์มหาวิทยาลัย
CHULALONGKORN UNIVERSITY

สาขาวิชา	วิศวกรรมไฟฟ้า	ลายมือชื่อนิสิต
	
ปี	2562	ลายมือชื่อ อ.ที่ปรึกษาหลัก
การศึกษา	
		ลายมือชื่อ อ.ที่ปรึกษาร่วม
	

6170372721 : MAJOR ELECTRICAL ENGINEERING

KEYWORD: Digital Image Processing, Avian Hematology, Blood Cell Counting

Tanapat Autaiem : Automatic Method for Avian Red Blood Cell and Heterophil Counting Using Iterative Thresholding. Advisor: Assoc. Prof. SUPATANA AUETHAVEKIAT, Ph.D. Co-advisor: Vera Sa-ing, Ph.D.

Thailand is one of the top broiler exporters. Red blood cell (RBC) and white blood cell (WBC) counting is one of the most basic methods for health screening process. Because the mammalian and avian blood is different, the mammalian blood analyzing techniques cannot be used, so the counting is done manually. This thesis proposes an automatic counting method for avian RBCs and heterophils, the most common type of avian WBC. The detection of avian RBC is challenging because of elliptic nucleated cell, the possibility of overlapped cells, and various staining. Otsu's multiple thresholding method is used to automatically extract nuclei under different staining. The threshold value is then reduced iteratively to separate connected nuclei. Heterophil detection is done by removing the detected RBCs, using edge information to extract possible WBCs, then applying statistically based algorithm to filter heterophils. The results show that RBC counting error is less than clinical acceptable error of 5% for 4 out of 5 types of slide and heterophil counting error is 8.8%.

CHULALONGKORN UNIVERSITY

Field of Study:	Electrical Engineering	Student's Signature
	
Academic Year:	2019	Advisor's Signature
	
		Co-advisor's Signature
	

ACKNOWLEDGEMENTS

I would like to express my sincere thanks to my thesis advisor, Assoc. Prof. Dr. Supatana Auethavekiat, for her help with this research and so many other things.

I would like to thank my co-advisor, Dr. Vera Sa-ing for his help with programming aspect and publication of this research.

In addition, I would like to acknowledge Dr. Khajornpong Nakgoi from Department of Livestock Development, Ministry of Agriculture and Cooperatives, Dr. Noppadol Prasertsincharoen and Dr. Peera Arreesnsom from Faculty of Veterinary Technology, Kasetsart University for cooperating, and providing data and samples for this research.

Finally, I would like to thank my family and my friends for all their support.

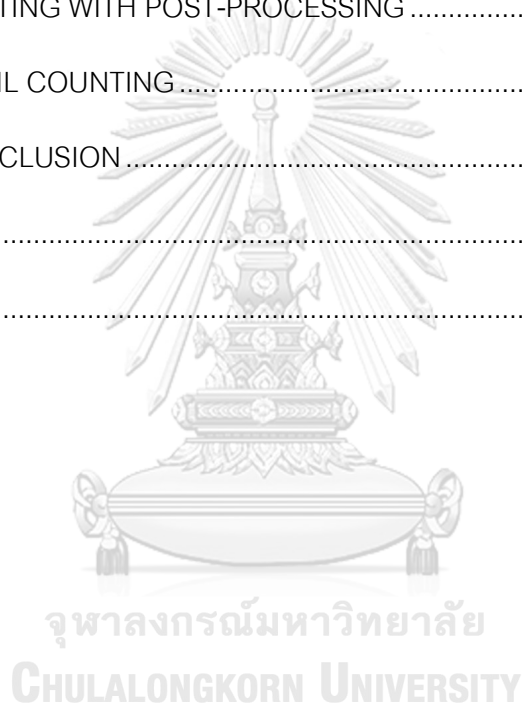
Tanapat Autaiem



TABLE OF CONTENTS

	Page
.....	iii
ABSTRACT (THAI).....	iii
.....	iv
ABSTRACT (ENGLISH)	iv
ACKNOWLEDGEMENTS.....	v
TABLE OF CONTENTS.....	vi
CHAPTER 1 - INTRODUCTION.....	1
1.1. PROBLEM STATEMENTS	3
1.2. SCOPE	3
1.3. CONTRIBUTION.....	4
1.4. RESEARCH PROCEDURE	4
CHAPTER 2 - RELATED WORKS.....	5
2.1. AVIAN WBC TYPE.....	5
2.2. AUTOMATIC MAMMALIAN RBC COUNTING.....	6
2.3. AVIAN RBC COUNTING	7
2.4. WBC COUNTING	8
2.5. OTSU'S THRESHOLDING.....	9
2.6. DBSCAN CLUSTERING	10
CHAPTER 3 - METHODOLOGY	12
3.1. NUCLEUS EXTRACTION	13
3.2. OTSU'S MULTIPLE THRESHOLDING.....	13

3.3. ITERATIVE THRESHOLDING.....	16
3.4. POST PROCESSING.....	17
3.5. HETEROPHIL DETECTION.....	23
CHAPTER 4 - EXPERIMENTS AND RESULTS.....	27
4.1. EXPERIMENT SETTING.....	27
4.2. RBC COUNTING.....	27
4.3. RBC COUNTING WITH POST-PROCESSING.....	30
4.4. HETEROPHIL COUNTING.....	34
CHAPTER 5 - CONCLUSION.....	36
REFERENCES.....	37
VITA.....	41



CHAPTER 1 - INTRODUCTION

Thailand is the tenth largest broiler producer in the world. It is the top exporter in terms of the weight of the processed chicken [1]. Health screening is one of the necessary quality control processes. One of the basic screening protocol is blood analysis. Despite the high market value, the automated cell counter of avian blood is not available. The blood analysis is performed manually. The manual process is both tedious and exhaustive.

The adaptation of human automated cell counter to avian blood is not a straightforward task, since the avian blood is far different from human (mammalian) blood. The avian red blood cell is nucleated and elliptic, whereas the human red blood cell is anucleated and circular. The sizes of avian red and white blood cells can also be comparable, while the size of the human white blood cell is much larger than the red one. Thus, the counting based on impedance and scattering is not appropriate. The existence of nucleus in the avian red blood cell (RBC) affects the accuracy of the white blood cell (WBC) counting by flow cytometry [2]. These problems may be overcome by the flow cytometry using immunophenotyping. However, the cost of developing reagents and antibodies, as well as the adoption of an automated cell counter in small farms is economically infeasible.

Image processing is an alternative and low-cost method for cell counting. Despite the difference in the visual properties of the avian and mammalian blood cells, the processing flow is the same. In case of the RBC count, first the input color image is converted to the grayscale image. Then, thresholding and noise reduction methods are applied to extract RBC. After that, the counting algorithm is applied. Mammalian circular RBCs can be effectively counted by applying circular Hough transform [3-5]; however, the detection of avian elliptic RBCs is much more complex than the circular one [6, 7]. Though, several automatic ellipse detection methods have been proposed [8-10], they

are complex and time-consuming. The problem is made more complicated because the cells may lie very close to one another, as shown in Figure 1. To overcome these two problems, many works suggest nucleus extraction instead of cell extraction. Using the fact that one RBC contains one nucleus and nuclei are not overlapped with each other, the number of nucleus region extracted should directly represent number of RBC. However, because there are at least three intensity regions in a slide (background, cytoplasm, and nucleus), the thresholding method needs to be more complex.

For WBC counting, most of the existing image processing methods is for mammalian WBC which cannot be directly applied to avian blood. Many works use color-based detection method [11-13] to extract WBC directly and completely ignore RBC. These works clearly would not work for avian case because the intensity of the nucleus in avian RBC is close to the nucleus of avian WBC. Furthermore, even though WBC of avian and mammal share similar appearance, their size when compare to RBC are different. Mammalian WBC is bigger than its RBC, but avian RBC is around the same size. Figure 2 shows said comparison of size and contrast between RBCs and WBCs of both avian and mammalian blood.

The objective of this thesis is to develop the method for counting avian RBCs and heterophils, the most abundant granulocyte in avian WBCs. Since the appearance of avian blood slides can be varied by different staining techniques as well as the staining time, the proposed method must be flexible and provide accurate counting under different staining techniques. However, our samples only have heterophils in one type of slide, so we do not consider flexibility for the counting of heterophils.

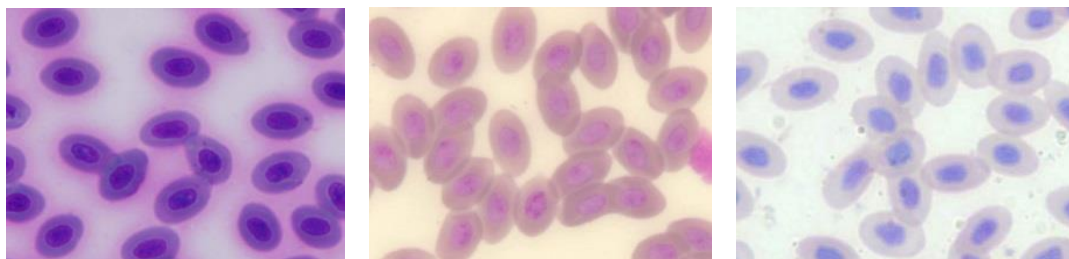
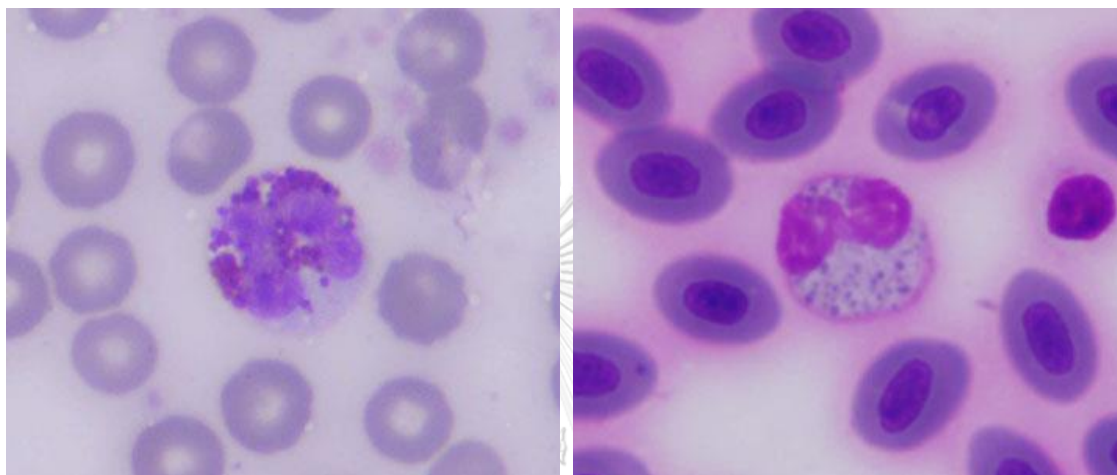


Figure 1. Avian blood slides examples



(a) Mammal (canine) blood cell (b) Avian blood cell

Figure 2. Comparison of mammal and avian blood cells

1.1. PROBLEM STATEMENTS

Three major problems need to be solved in automatic avian RBC counting: (1) oval and nucleated red blood cell, (2) overlapped cells, and (3) non-uniform staining, varying staining color, and appearance.

The characteristics of heterophils need to be extracted in order to differentiate between the heterophil and other tissues in the slides.

1.2. SCOPE

1. The proposed algorithm is applied only to the blood samples taken from healthy chickens (*Gallus gallus domesticus*).
2. The proposed algorithm is applicable only to the staining whose cell nucleus is apparent.

3. At least 5 different staining appearances were used in the experiment for red blood cell counting.
4. Only one staining type is used for heterophil counting.
5. The gold standard of the cell counting comes from manual counting.

1.3. CONTRIBUTION

1. A system that is capable of counting avian red blood cell and robust to different staining types.
2. An algorithm for automatically detecting heterophil, the most common type of avian white blood cells.

1.4. RESEARCH PROCEDURE

1. Literature review on blood counting algorithm.
2. Design and implement the proposed algorithm.
3. Evaluate and improve the proposed algorithm.
4. Check whether the conclusions meet all the objectives of the research work of the dissertation.
5. Write the dissertation.

Research Procedure	2019					2020					
	Aug	Sep	Oct	Nov	Dec	Jan	Feb	Mar	Apr	May	Jun
1. Literature review											
2. Design and implement the proposed algorithm											
3. Evaluate the proposed algorithm											
4. Write the dissertation											

Figure 3. Gantt chart

CHAPTER 2 - RELATED WORKS

2.1. AVIAN WBC TYPE

There exist 5 WBC types in avian [14]: heterophil, eosinophil, basophil, monocyte and lymphocyte. The appearance and the functions of each type is as follows.

- Heterophil is not found in mammal but can be considered equivalent to the neutrophil. It is the most common WBC in avian. It has two or three nuclei and is packed with rod shaped granules as shown in Figure 4(a). It is produced to fight the inflammation and is phagocytic.
- Eosinophil is granular and its appearance varies among avian species. It is quite similar to the heterophil; however, its granule in most species has different staining color (Figure 4(b)) and is round. The increase in eosinophil may indicate the parasitic infection.
- Avian basophil has different appearance from the mammalian one. It is granular but its granules are dissolved by alcohol-based stain. Its nucleus is often hidden by granules as shown in Figure 4(c). Its function is believed to be the same as the mammalian counterpart, i.e. to fight allergy and infection.
- Monocyte has only one nuclear. The shape of its nuclear varies among species from round to horseshoe shape (Figure 4(d)). Like its mammalian counterpart, its function is to fight the foreign organism and remove dead and damaged cells.
- Similar to monocyte, a lymphocyte is a mononuclear WBC. However, as shown in Figure 4(e), the ratio between the nucleus and cytoplasm is higher than monocyte (Figure 4(d)). However, the ratio varies among avian species and cannot be used as a universal criterion. Its appearance can also be similar to platelet. Avian lymphocyte has similar function to the mammalian one and is important to the immune system. The high number of the lymphocyte indicates the infection.

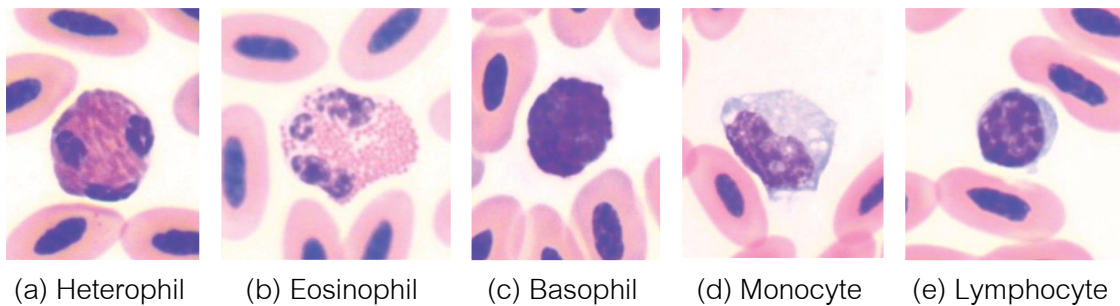


Figure 4. Avian WBC Types [14]

2.2. AUTOMATIC MAMMALIAN RBC COUNTING

Though the algorithm to detect mammalian RBC can be varied, most of them share the same processing flow [3]. Figure 5 describes general flow of mammalian RBC counting. First, the pre-processing is used to enhance a slide image. The color slide image is converted to the gray-scaled image and thresholding is applied to remove the background. The RBCs is the major part of the slide, and the WBCs occupy only small area. So, the effect of the much darker WBC (as shown in Figure 2) can be ignored. Conventional thresholding methods, such as Otsu's thresholding, is effective for this task.

After the background has been removed, the remaining areas are mostly RBCs but it may also contain a few WBCs, platelets and staining color blot. The circular shape of mammalian RBCs are easy to detect, so the most common strategy for RBC detection is the application of circular detection algorithm.

Circular Hough transform is a simple and effective circular detector. It is widely adopted for mammalian RBC counting [3]. Maitra et al. [4] and Mazalan et al. [5] have different pre-processing but both use circular Hough transform. For pre-processing, the former uses edge detection, spatial smoothing filtering, and adaptive histogram equalization while the latter uses morphological process. Both works show remarkable results. Though RBC is circular, its shape may not be a complete circle due to the cell overlapping or at the boundary of the image. Care must be taken to set the sensitivity of

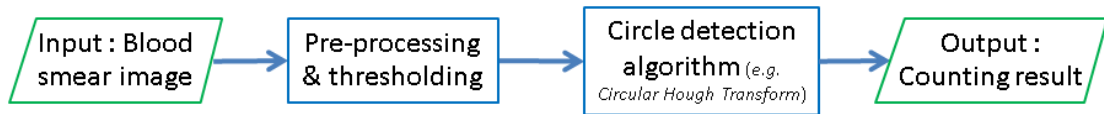


Figure 5. General mammalian RBC counting flowchart

the circular Hough transform to ensure that the detection is sensitive enough to detect the overlapped and incomplete RBCs, but not too sensitive to include other tissues or noise into the counting. To solve the difficulty in parameter setting, Autaiem et al. [15] applies the circular Hough transform twice. First, the circular Hough transform is applied with low sensitivity to count individual RBCs (complete circle). Then the circular Hough transform is reapplied with high sensitivity to count the clustered or incomplete RBCs.

2.3. AVIAN RBC COUNTING

An ellipse is much more difficult to detect than a circle since it is directional orient and the ratio between the minor and the major axes can be varied. Since the nucleus is distinct from the cytoplasm and there is only one nucleus per one RBC, the detection of avian RBC is usually based on the nucleus [16-18] instead of the shape.

Beau-frère et al. [16] applied CellProfiler, an open-source image processing software (available for download at <https://cellprofiler.org/>), to count RBCs. First, the robust background thresholding method is applied to extract RBC nuclei. Then the machine learning is used to extract and count the nuclei. However, we failed to replicate similar results with our samples which contain slides with different staining techniques. So, we conclude that this method has low flexibility when it comes to different samples.

Meechart et.al. [17] proposed the double thresholding method for extracting the nucleus of avian RBCs. Otsu's thresholding [19] is first applied to separate the gray-scaled slide image into cell and background regions. Otsu's thresholding is then reapplied to only the cell region to find the threshold, T_2 . The threshold used to separate cell to cytoplasm and nucleus is set as γT_2 , where γ is the user defined

constant ($0 < \gamma < 1$). The detected nuclei region is denoised by morphological opening operator. Their method is simple and required only one user defined parameter; however, its accuracy is greatly affected by staining techniques.

Recently, Ochoa et al. [18] proposed Mizutama, the software which can accurately count both non-nucleated and nucleated RBC. They use multiple thresholding to separate RBC into cytoplasm and nuclei regions. Then, various measurements are performed to rule out non-RBC. However, five parameters need to be manually calibrated. The method is not user-friendly as staining techniques can be varied in case of counting avian RBCs.

2.4. WBC COUNTING

Since a mammalian RBC does not have a nucleus, a number of automatic detection of mammalian WBCs starts with the detection of the nucleus [11-13]. Liu et al. [11] proposed a robust segmentation method using nucleus mark watershed operations and mean shift clustering. The nuclei are obtained via the information of rg chromacity space and HSI color space. The nuclei are used as seeds to extract WBCs by the following process. First, mean shift clustering operation is applied. The C component of CMYK color space is extracted and enhanced by various techniques. After that, the nucleus mark watershed operation is used to separate adhesive cells. The method is robust and provides great performance.

Tareef et al. [12] proposed a segmentation method with color and texture-based image enhancement. To detect nucleus, RGB and CIE LAB color spaces are used to create enhanced gray-scale image, which is then thresholded using Poisson distribution based minimum error thresholding algorithm. To detect cytoplasm, an enhancement procedure based on discrete wavelet transform and morphological filtering is used to increase the contrast of cytoplasm, which is then extracted using Otsu's thresholding.

Finally, the cells are refined using distance regularization and morphological operations. The method provided good cytoplasm segmentation.

Ahasan et al. [13] proposed a segmentation method for blood smear with normal and leukemia condition. Color thresholding with CIE LAB color space is used to obtain RGB mask image, then the mask image is thresholded using Otsu's method. After noise reduction by using averaging filter, marked controlled watershed algorithm is performed to separate connected WBCs. Finally, platelets area and megakaryocytes are removed using area removal technique and broken WBC is reconstructed using morphological closing. The method gave overall 88.57% accuracy and could be improved to cover other disease conditions.

Liu et al. [20] proposed a detection method based on cue location given by edge density and color contrast, followed by segmentation which is done using iterative GrabCut algorithm to extract WBC region. However, the work is for mammalian blood and limits the number of WBC to only one per slide. Nonetheless, this is one of many works we think would be possible to apply for avian blood because the concept of using edge information is not depended on using the said different of size and color.

2.5. OTSU'S THRESHOLDING

Otsu's thresholding [19] is one of the most basic automatic thresholding methods. The classic Otsu's thresholding automatically separates image into two categories, background and foreground. The threshold value is determined by minimizing intra-class variance (Equation (1)), or equivalently, maximizing inter-class variance.

$$\sigma_W^2 = \omega_0\sigma_0^2 + \omega_1\sigma_1^2 \quad (1)$$

where σ_W^2 is the intra-class variance, ω_i and σ_i^2 are probability and variance of class i respectively.

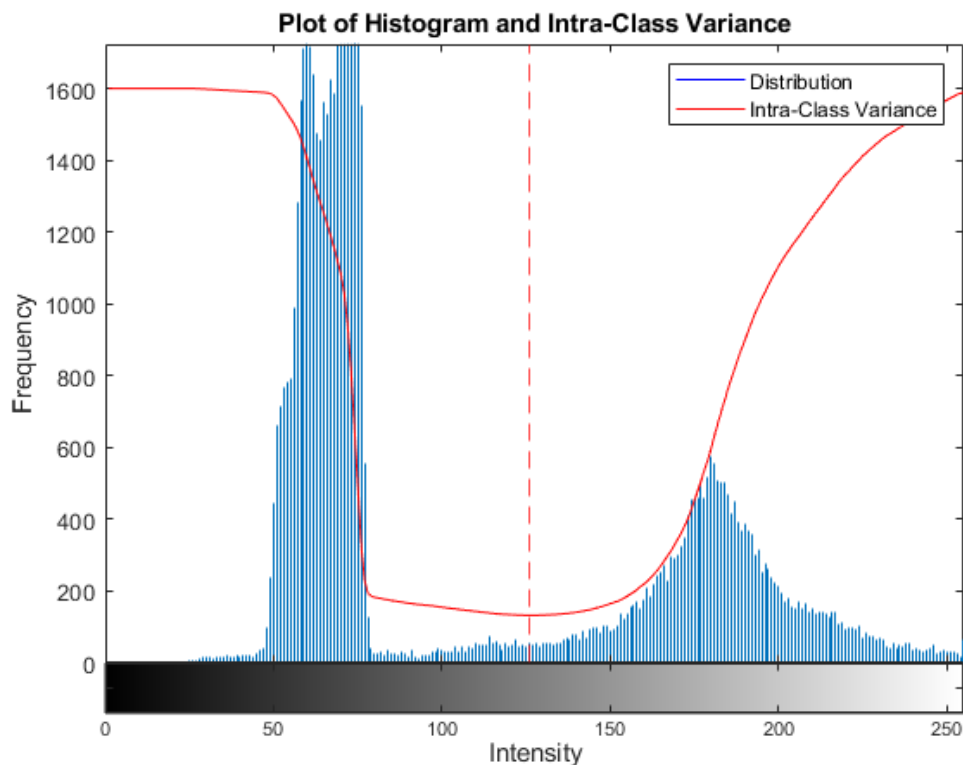


Figure 6. Otsu's Thresholding and Intra-Class Variance

Figure 6 shows an example of histogram of two-category data overlay with scaled its intra-class variance. The correct threshold (red dashed line) leads to a low intra-class variance (red line). While the incorrect threshold leads to higher intra-class variance. Otsu's thresholding can be easily adapted for the segmentation of more than two categories. The threshold is set to maximize inter-class variance.

2.6. DBSCAN CLUSTERING

Density-based spatial clustering of applications with noise (DBSCAN) [21] is simple and, unlike many other classification tools, does not require the number of classes as the prior information (e.g. k-means clustering). It uses two predefined parameters: epsilon and the minimum number of epsilon neighborhood point (minpts). These two parameters are used to discover clusters from noise. Epsilon is the distance threshold value which is used to classify whether the nearby points are epsilon neighborhood points or not. Distance metric used in DBSCAN is selected based on the

target application. The selection for these 2 parameters in our work is described in detail in Section 3.4 of Methodology chapter.

The points that have the number of epsilon neighborhood points equals to *minpts* or larger are assigned as “core points” of the cluster. The points that have the number of epsilon neighborhood points less than *minpts* but are one of the epsilon neighborhood points of some core points are assigned as “border points” of the cluster; otherwise, are considered “noise points”. Below is the algorithm summary of DBSCAN that is implemented in MATLAB as the “*dbscan*” function [22] :

1. From the input data set, \mathbf{x} , select the first observation point \mathbf{x}_i .
2. Find the epsilon neighborhood points of \mathbf{x}_i (the points within *epsilon* distance).
 - a. If the number of epsilon neighborhood points is less than the specified *minpts*, then label \mathbf{x}_i as a noise point. Otherwise, label \mathbf{x}_i as a core point of cluster \mathcal{C} .
 - b. For each neighborhood points of the core point, find its epsilon neighborhood points. If the number of epsilon neighborhood points is less than *minpts*, it is labelled as a border point. Otherwise, it is a core point. In this step, if the noise point is the neighbor of a the newly assigned core point, it will become a border point.
 - c. Repeat Step b. until there is no neighbor assigned as a core point.
3. Select the next unlabeled point, then repeat Step 2. If new core point is found, label it as the new cluster. Repeat until there is no unlabeled point.

In DBSCAN, the parameter space for clustering as well as the distance metric are arbitrary. DBSCAN is very general and great for discovering cluster and noise in data. However, it has limitations when dealing with data with varying densities and data with high dimensional feature spaces.

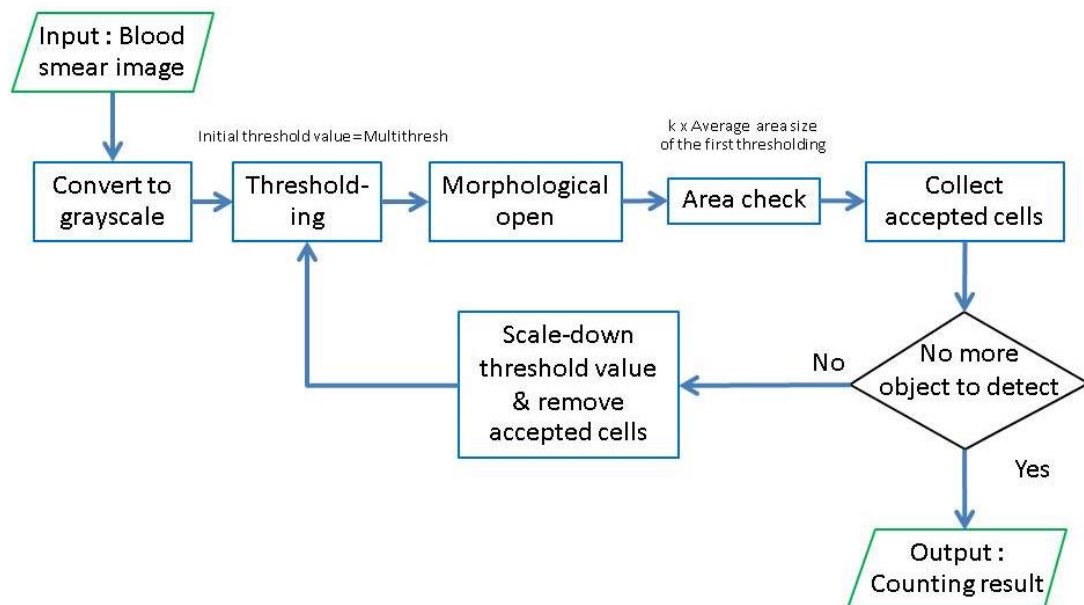


Figure 7. The flowchart of iterative thresholding method for avian RBC counting

CHAPTER 3 - METHODOLOGY

Blood analysis consists of counting both red and white blood cells. Compared to red blood cells (RBC), the number of white blood cells (WBC) is very low. In this thesis, we have enough data only to detect heterophils. The proposed method is divided into two stages. In the first stage, the RBCs are counted and removed from the slide. In the second stage, the heterophils are detected from the remaining area. Rule based algorithm is used to differentiate the heterophil from the rest.

There are three major obstacles in the automatic avian RBC counting: elliptic RBCs, overlapped cells and varying staining techniques. Furthermore, within a slide, the staining color is not uniform. The non-uniform staining will be described in Otsu's multiple thresholding section.

Figure 7 depicts the overall process of our proposed RBC counting method, the iterative thresholding method.

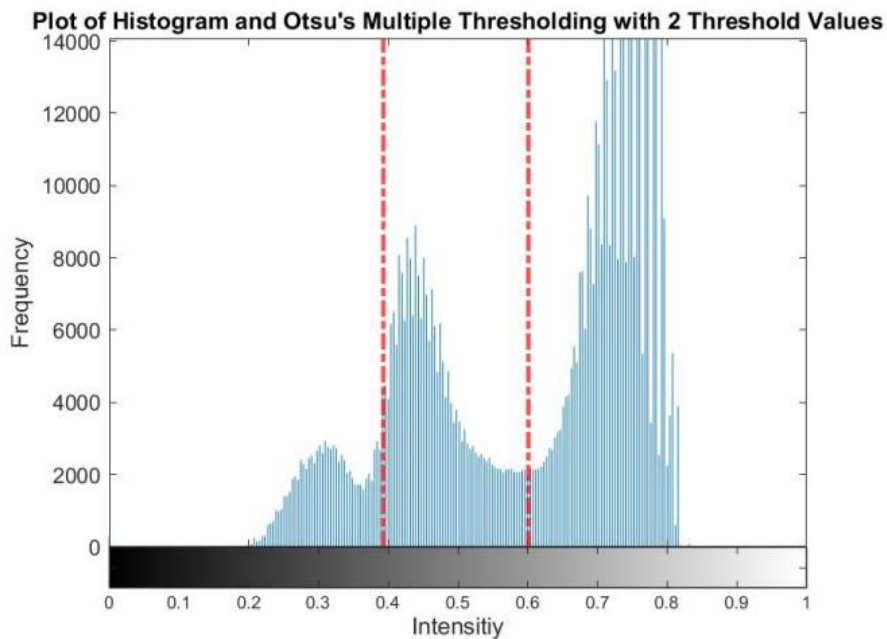
3.1. NUCLEUS EXTRACTION

Cell nuclei are not overlapped even when the cytoplasm does and they are separated by cytoplasm; therefore, the general strategy to deal with the elliptic RBC shape and the overlapped cells is to extract and count nuclei. One RBC contains one nucleus, so the number of nuclei directly represents the number of RBC. The RBC counting problem is changed to the nucleus detection. One way to extract the cell nuclei is to simply use a general automatic thresholding method to find a value that separates RBCs and background, then downscale the value with experimentally set constant. However, the constant may need to be changed if the slide images are different in color, which corresponds to the different staining problem. For a method to be more flexible, it is better to find a way to get threshold value that directly extract nucleus.

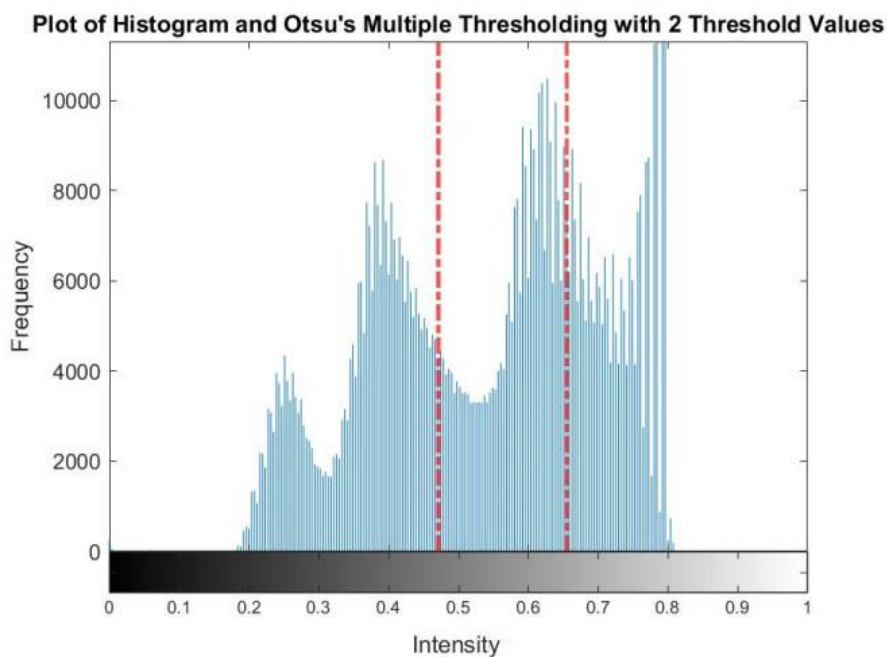
After thresholding, the noise reduction technique is performed. In this work, we use morphological opening and a disk as a structure element. In image morphology [23], there are two main operators: dilation and erosion. The binary image is translated according to the shape of structure element. The dilation and the erosion operators are the union and the intersection of translated images, respectively. In morphological opening, the erosion operator is applied before the dilation operator, i.e. shrink then expand. The results are that small noises are removed and object's contour becomes smoother.

3.2. OTSU'S MULTIPLE THRESHOLDING

We choose Otsu's multiple thresholding [19] to cope with the problem of different staining color. Ideally, a slide image is divided into three regions: background, cytoplasm, and nucleus. However, the investigation of the histogram of actual slides reveals that one slide may contain more than three distinct brightness groups. Therefore, the segmentation of a slide image to three regions leads to incorrect segmentation as demonstrated in Figure 8. We call the problem that different slides may have different intensity distribution as 'inter-slide non-uniform' staining problem.



(a) Correctly segmented image



(b) Incorrectly segmented image

Figure 8. Examples of image histograms when the images are correctly and incorrectly segmented into three regions. The incorrect segmentation is due to inter-slide non-uniform problem. Red dotted lines show the threshold value.

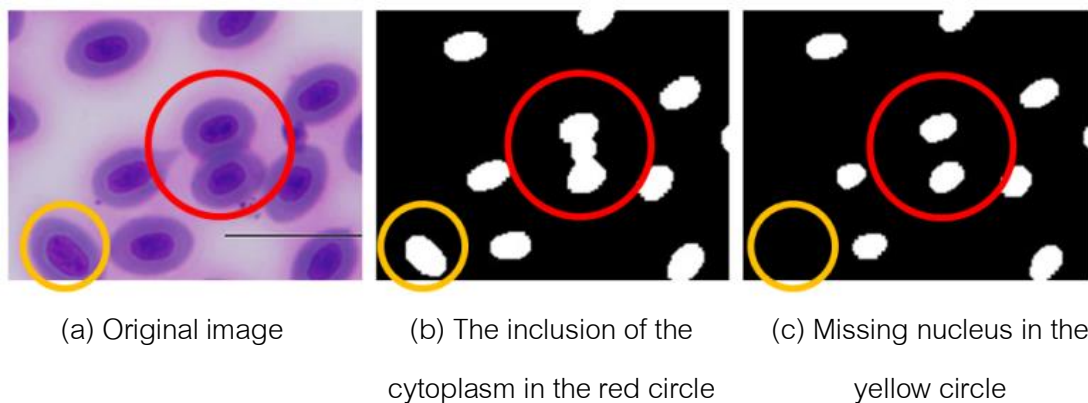


Figure 9. Example of false nucleus detection

Furthermore, even if the threshold value is correctly selected, there exists a problem where a threshold value that works for one area does not work for other areas in the same slide as shown in Figure 9. It can be seen that the nucleus in the lower left corner (orange circle) is correctly extracted. However, the overlapped cytoplasm of the two cells (red circle) is incorrectly included in the result, as shown in Figure 9(b). This problem can be partially solved by reducing the threshold value, but the smaller threshold leads to the removal of the nucleus in the lower left corner as shown in Figure 9(c). We call this 'intra-slide non-uniform' staining problem.

Figure 8(b) indicates that the cause of inter-slide non-uniform problem is that one slide may contain more than three regions. To deal with this problem, it is necessary to determine the number of regions within an image that provide the consistent result. The number is determined by experiment. The experiment on 30 slides revealed that the segmentation to five regions provided the consistent threshold values (Figure 10). User needs to determine only which threshold value (among the four values) should be used for nucleus extraction.

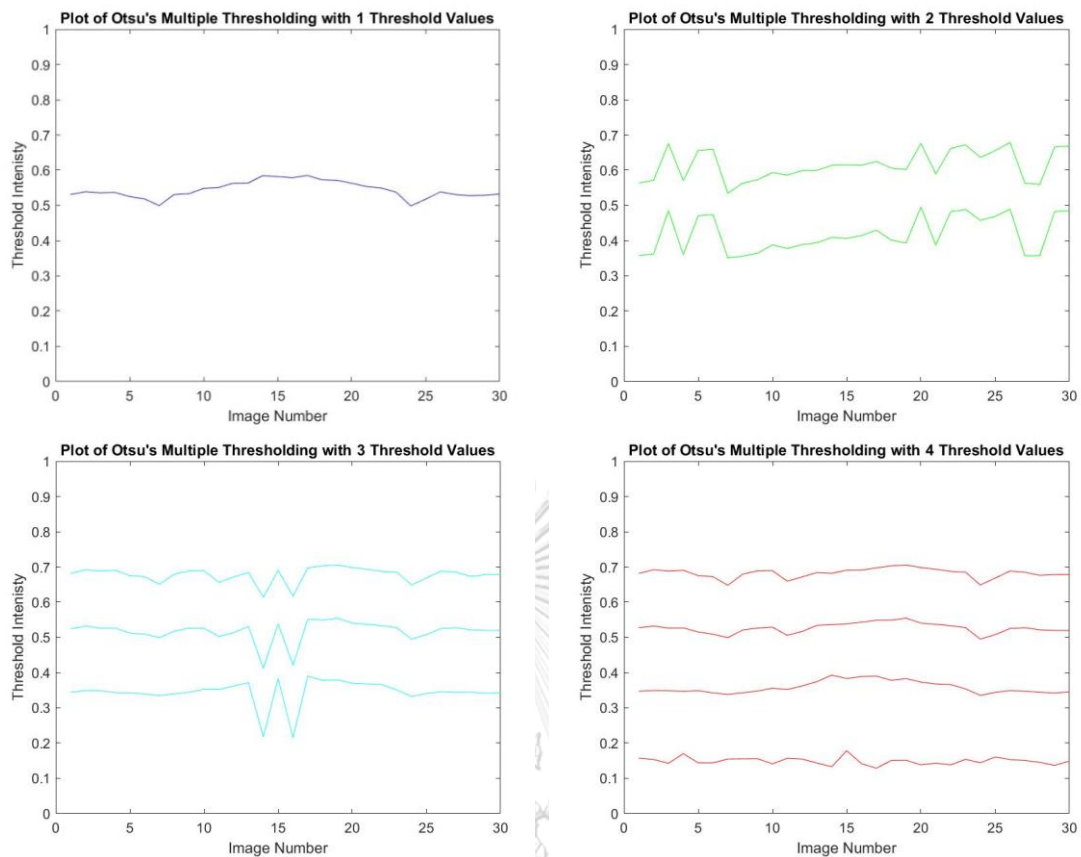


Figure 10. Graph showing the Otsu's threshold of 30 slides when the number of regions is varied.

3.3. ITERATIVE THRESHOLDING

Otsu's threshold is the global threshold and estimated from an entire image. Thus, it is affected by the intra-slide non-uniform staining problem. In order to cope with this problem, the thresholding is performed iteratively, with the Otsu's threshold as the initial threshold value.

In each iteration, a possible nucleus is extracted as the region whose intensity is lower than the threshold, which is estimated in the previous iteration. The morphological opening is then applied to remove noise. Then the area of each possible nucleus is estimated. The possible nucleus is 'accepted' as the actual nucleus, if its area is lower or equal to k times of the average area size. The accepted nuclei are collected and removed. The threshold value is then reduced (to be used as the threshold in the

subsequent iteration). The process is iterated until there is no possible nuclei region left. Figure 11 shows the example of the nuclei detected in each iteration.

The optimal value of k is set by experiment. If k is set too high, the iteration will stop prematurely; consequently, some nuclei will not be counted. On the other hand, if k is set too low, non-nucleus and noisy regions will be included as the actual nuclei. Figure 12 shows the percent counting error when k is varied. Figure 12(a) shows the average error of the 30 slides used in setting the number of regions within an image. Since 5% counting error is acceptable in clinic, the result indicated that the k value should be set to 0.7 or higher. The effect of too high k is not distinct in this graph. So, we perform another experiment on the slide with different staining technique. The result is as shown in Figure 12(b). The k value providing the acceptable result is between 0.9 and 1.5. For simplicity, we choose 1.0 for the value of k in the subsequent experiments. Note that the two types of slide are referred as Type-1 and Type-2 in the result section. Refer to Figure 13 for the appearance of Type-1 and Type-2 slides.

3.4. POST PROCESSING

In the iterative thresholding, nuclei are detected based on the intensity and the size. However, the intensity and the size are not the unique properties of an RBC nucleus. Some objects are incorrectly detected as the RBC as shown inside the yellow circle in Figure 14(a). To differentiate between the real nuclei and the incorrectly detected objects, additional information besides the nucleus is required. The cytoplasm around the RBC nucleus is lighter than the nuclei, but still darker than most regions in the slide. Furthermore, compared to a granulocyte, the RBC has smoother cytoplasm. Therefore, the area around the nuclei are extracted and used to differentiate between the red blood cells and other tissues/artifacts.

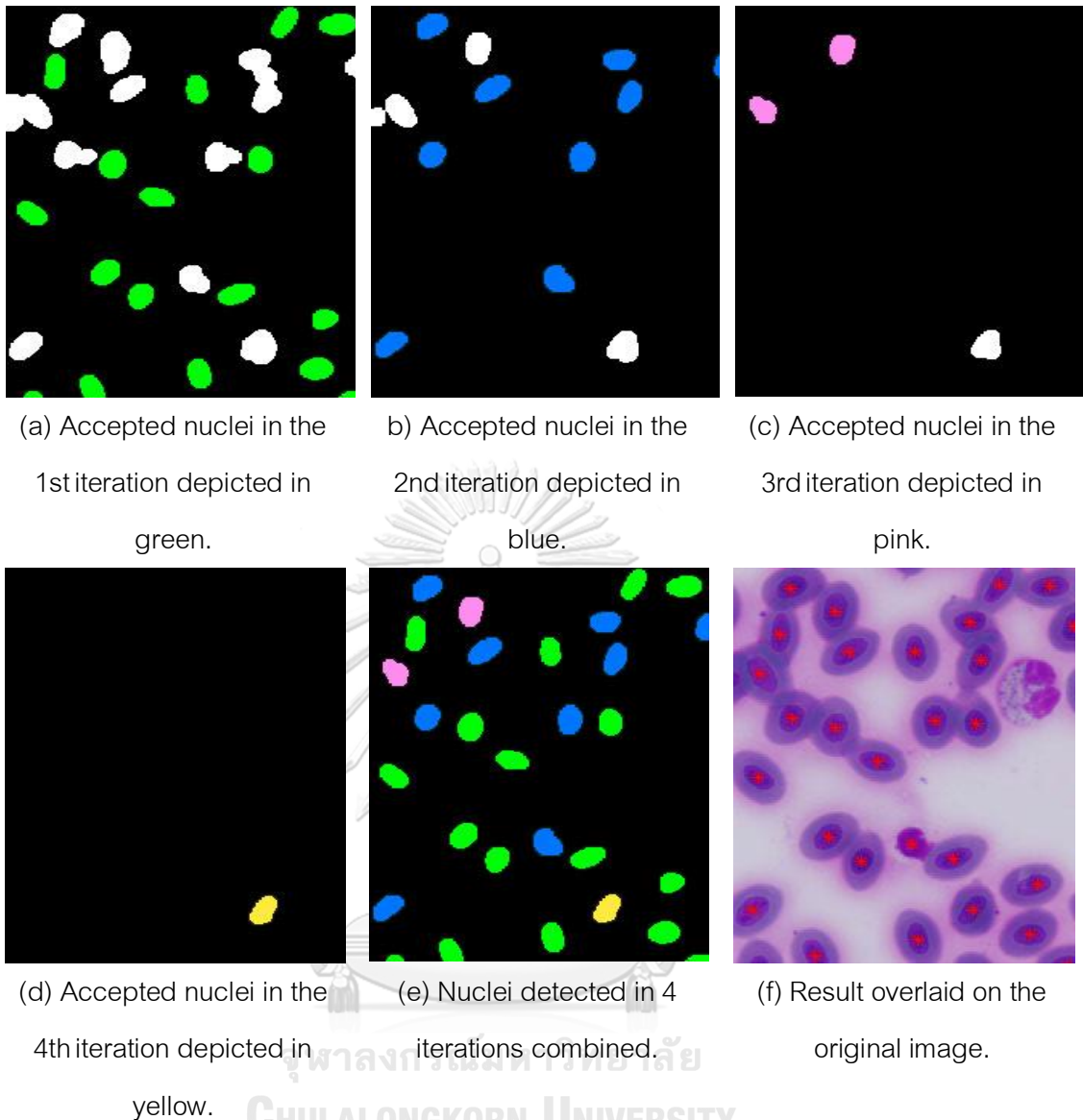
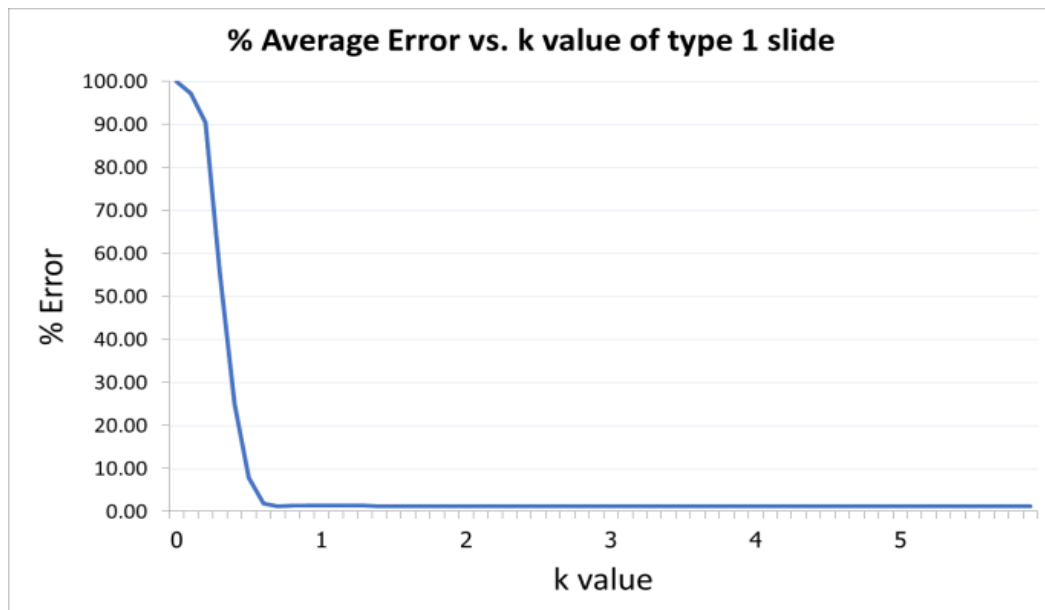
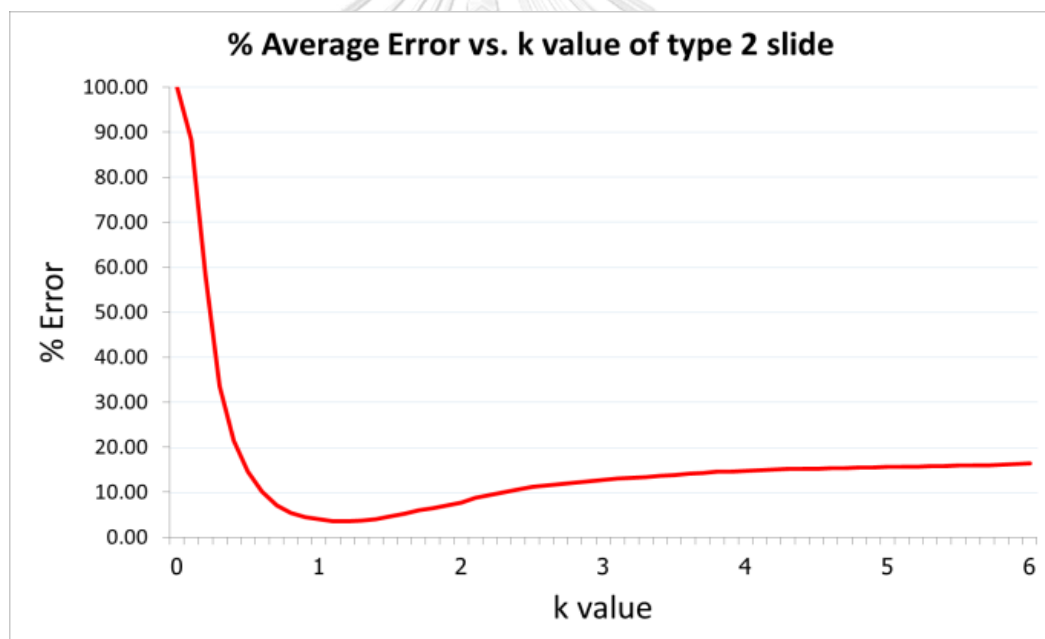


Figure 11. The nuclei detected in each iteration and overall result of our proposed method.

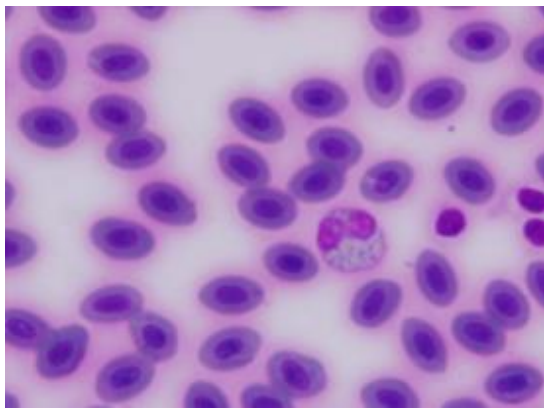


(a) Average Error vs. k value of Type-1 slide. (acceptable range is more than 0.7)

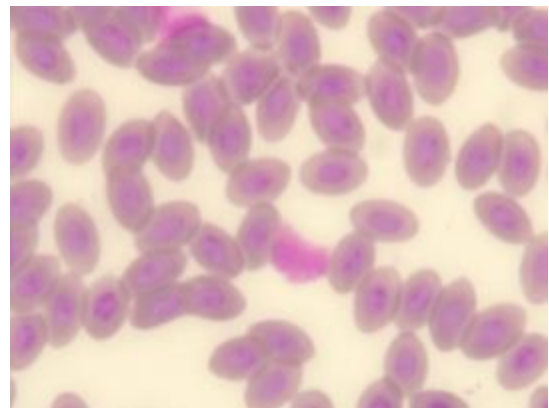


(b) Average Error vs. k value of Type-2 slide. (acceptable range is between 0.9 and 1.5)

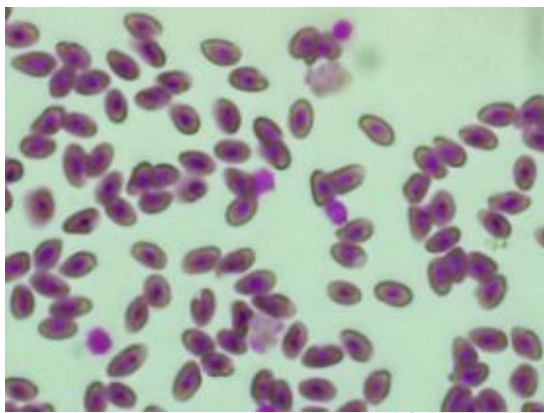
Figure 12. Percent average error vs. k value of type 1 and type 2 slides.



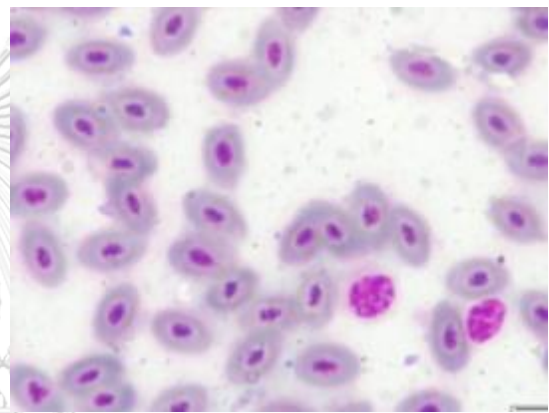
(a) Type-1 slide.



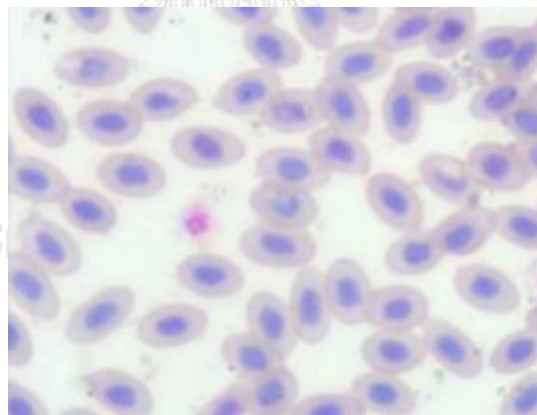
(b) Type-2 slide.



(c) Type-3 slide.



(d) Type-4 slide.



(e) Type-5 slide.

Figure 13. Example of 5 different appearance of RBCs used in the experiment.

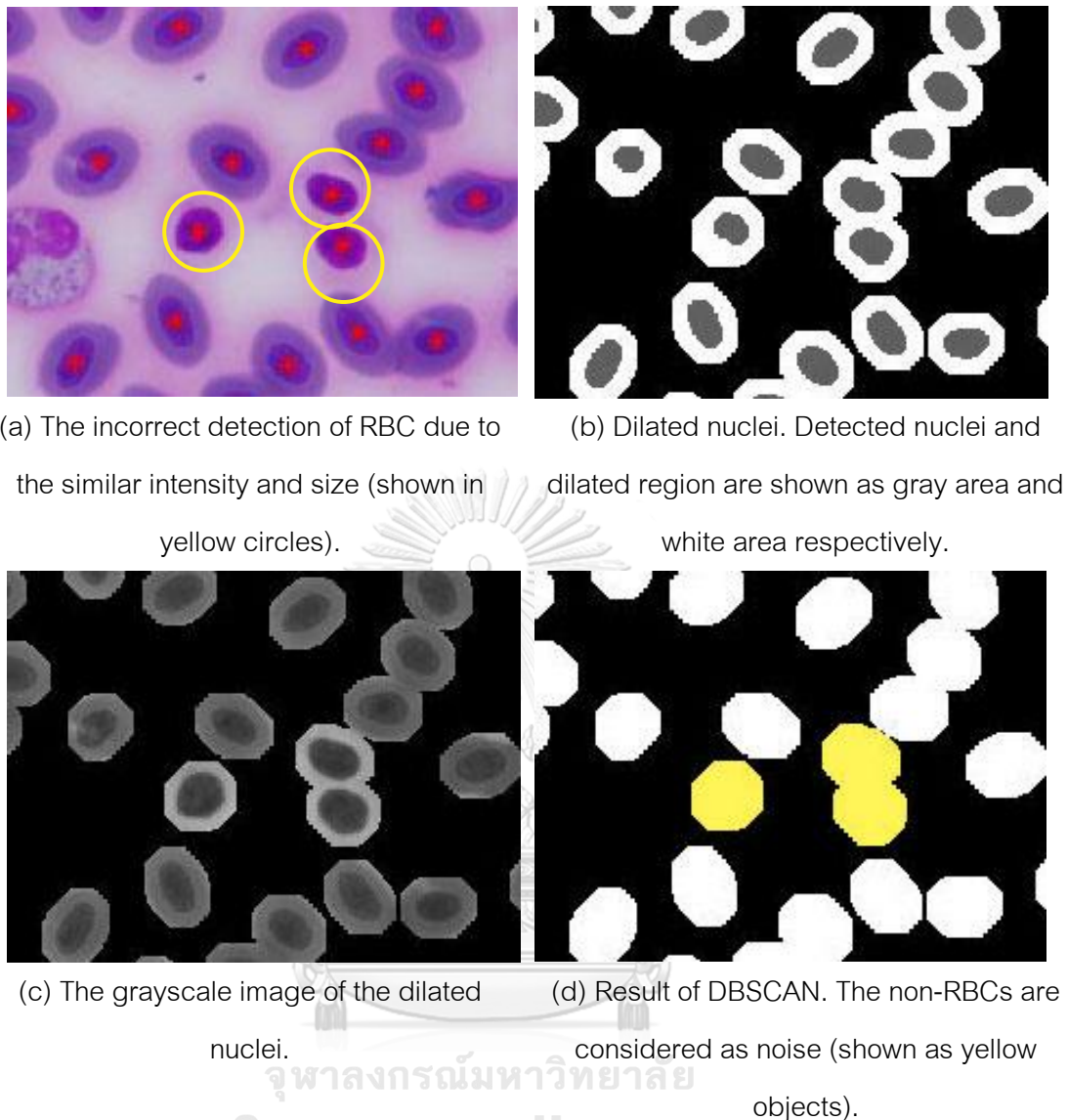


Figure 14. Post-processing steps

To obtain information of the surrounding region, morphological dilation is applied to the result of the iterative thresholding (Figure 14(b-c)). The intensity mean and variance of both the detected objects and the surrounding region (4 parameters) are used to describe the relative brightness and the intensity homogeneity, respectively. These four parameters are clustered into noise (small regions) and actual objects (RBC) by applying DBSCAN [21]. In this thesis, we use the default setting for distance metric which is Euclidean distance.

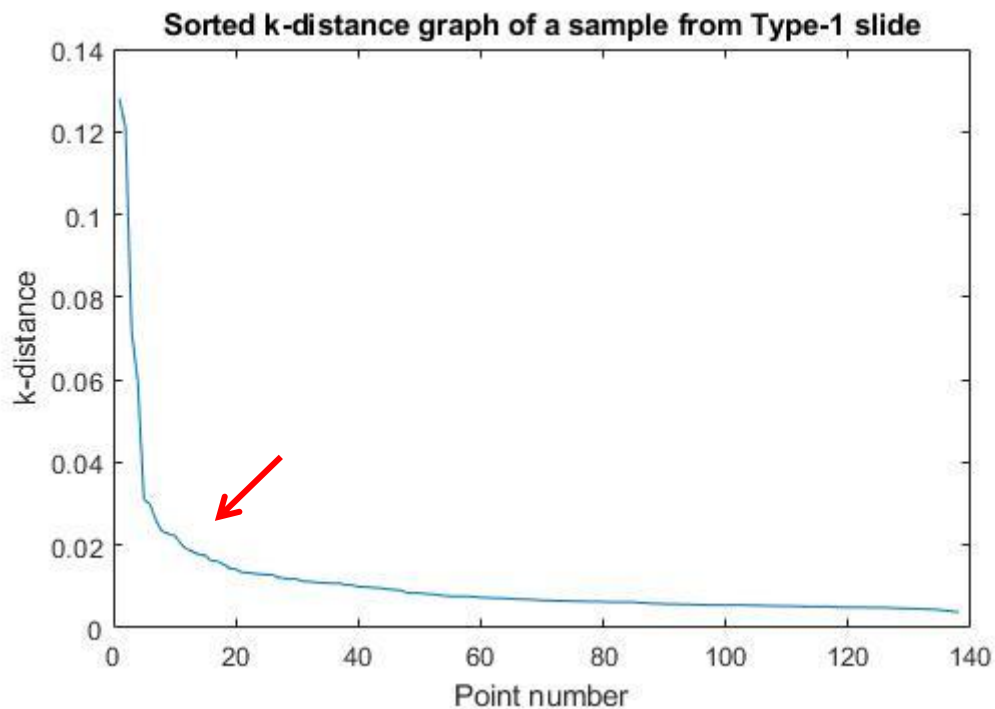


Figure 15. Sorted k-distance graph that is used for epsilon selection.

We simply choose the cluster with the highest number of points as RBC and the rest as non-RBC. This method is appropriate for our sample, as the detected objects cannot simply be classified into 2 classes: RBC and non-RBC, because the non-RBC can be many things such as white blood cells, color staining, platelets, etc. Figure 14(d) shows clustered non-RBCs which are considered as noise by DBSCAN.

Note that we use $\epsilon = 0.03$ and $\text{minpts} = 10$ in this research. These two parameters are selected according to the strategy suggested in [21]. In short, the minpts value should be equal or more than $p+1$, where p is the number of dimensions of the input data. And ϵ is determined by plotting the sorted k-distance graph, where k is minpts , then finding the distance value at the first “valley” of the graph, as shown by red arrow in Figure 15.

3.5. HETEROPHIL DETECTION

After the post processing, it is assumed that the position of every RBC is known. We can use this information to remove RBC from further process, and design the algorithm to differentiate heterophils from other non-RBC objects (other type of WBC, staining color, platelets, background slide...) We divide the heterophil detection into 2 stages: the possible WBC detection and the rule-based algorithm to detect the heterophil.

Although the relative size of a WBC and an RBC in avian is different than the one in mammal¹, the appearances of the WBC in avian and mammal are similar. We investigate the criteria for the mammalian WBC detection that is not based on the size difference. Note that the methods based on machine learning are not appropriate due to the limited number of available images. Edge density and color contrast have been successfully applied to detect the WBC in [20]. The edge density of Figure 16(a) is shown in Figure 16(b). The figure indicated that the maxima (brightest region) is the location of the WBC (shown by the yellow arrow). However, the boundary is blurred due to the interference from the edge of both RBC and WBC. It is difficult to set the threshold to extract the accurate boundary. The color contrast (Figure 16(c)) does not provide any clue to detect the WBC and cannot be used in our works. Note that the RBC shows the strong response (bright region) in the color contrast due to the presence of its nucleus. Iterative GrabCut algorithm is employed in [20] to detect WBC under the assumption of one WBC per image. The GrabCut algorithm is not adopted in our works, because this assumption can be violated.

¹ The size of an avian WBC can be comparable the one of a RBC; however, the size of a mammalian WBC is much bigger than the one of a RBC.

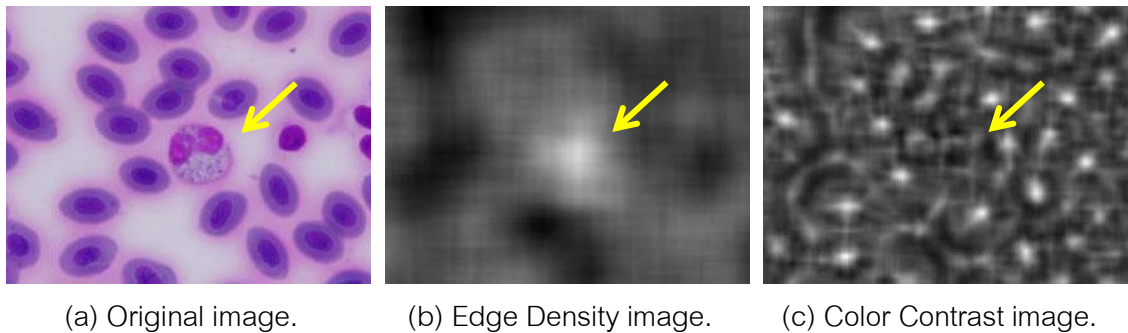
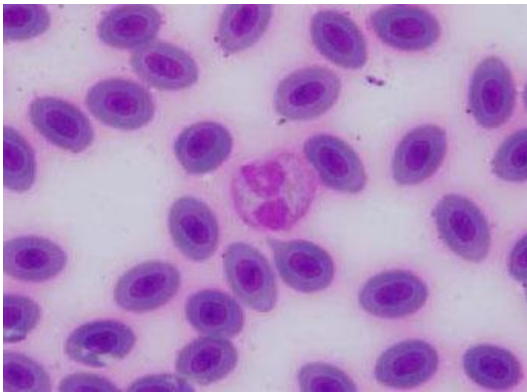


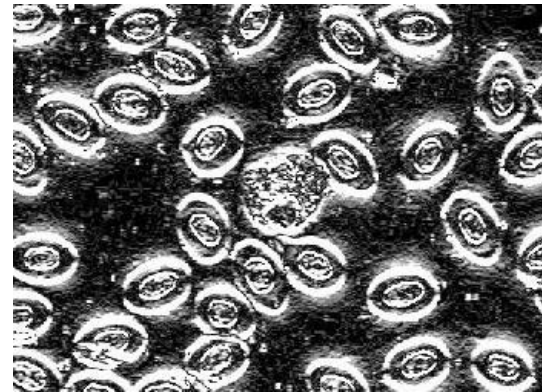
Figure 16. Implementation of [20]

Since the position of WBC can be inferred from the edge information. We design the algorithm for possible WBC detection by combining the Sobel edge detection with the conventional Otsu's thresholding. Figure 17 shows the result of each step in our process. First, the Sobel edge detection is applied to the gray scaled image of the slide and the result is shown in Figure 17(b). The result is binarized by using manually fixed threshold (Figure 17(c)). All RBC are removed to reduce their interference to the final detection. Morphologically closing followed by opening is applied to smooth the result (Figure 17(d)). Though the WBC has been located, it is not guaranteed to be a complete cell. Some nuclei are missing due to its fairly uniform intensity distribution. The missing nuclei can be retrieved from the result of the binarization by applying the conventional Otsu's thresholding (Figure 17(e)). The areas of the detected RBCs are removed from Figure 17(e). Finally, we combine the non-RBC regions in Figure 17(e) with Figure 17(d) to form the complete WBC (shown in red in Figure 17(f)).

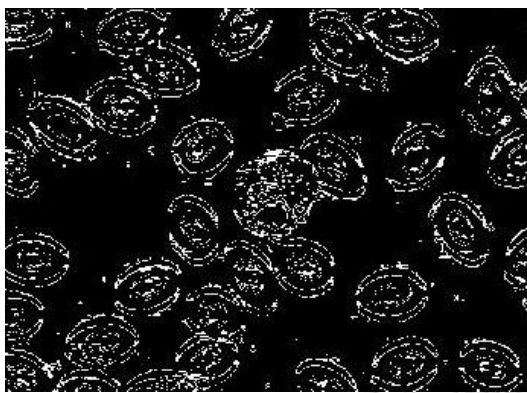
After detecting possible WBC objects, we use a simple rule-based algorithm to detect heterophils. The values used in our rules are a cell size, the percent of cytoplasm area, and the percent of nucleus area. The heterophil detection is designed for only one staining color so the cytoplasm and the nucleus area can be extracted by the fixed threshold. In this thesis, all thresholds are set by examining every heterophils in Type-1 slide (30 slides in total and approximately one heterophil per slide). Intensity range of cytoplasm and nucleus are determined by skimming through said regions with a pixel intensity visualizing tool and found to be 0.4-0.7 and 0.3-0.5, respectively.



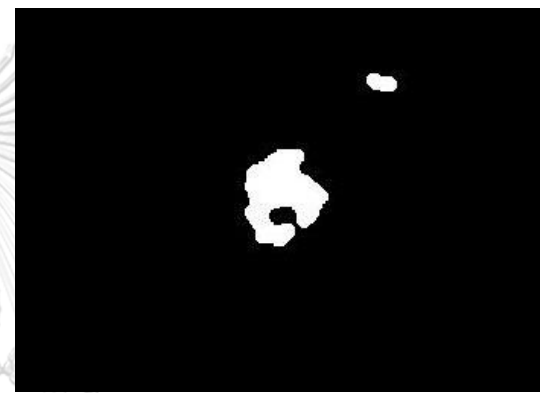
(a) Original image.



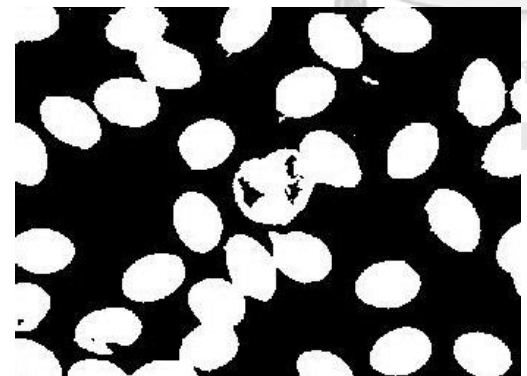
(b) Sobel image.



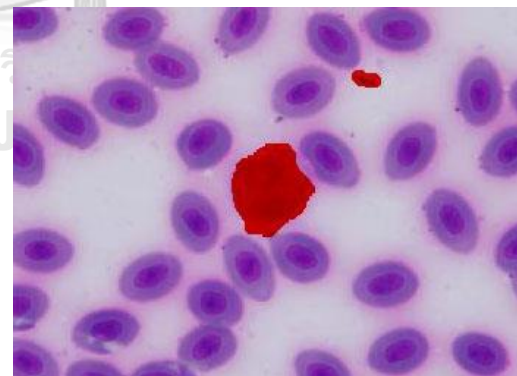
(c) Thresholded Sobel image.



(d) Thresholded Sobel image without RBCs region after Morphological closing and opening.



(e) Binary image of (a) by using Otsu's thresholding to its gray scaled image.



(f) Combined Sobel and Otsu image without RBCs region, then overlay on the original image.

Figure 17. The result of each step in the proposed algorithm for the detection of possible WBCs

The statistics of heterophils are shown in Table 1. Note that the summation of the percent of cytoplasm and the one of nucleus area is larger than 100%, because of the overlapped intensity range (0.4-0.5). The following four rules are used to detect the heterophil.

- (i) The size of a heterophil is larger than 3500 pixels.
- (ii) The cytoplasm of a heterophil has the intensity between 0.4 and 0.7 and covers more than 50% of the total area.
- (iii) The nucleus of a heterophil has the intensity between 0.3 and 0.5 and covers between 15% to 80% of the total area.
- (iv) The size of a heterophil is not larger than 8000 pixels. If the size of the detected heterophils is larger than 8000, the detected area consists of two heterophils.

The four rules are summarized in Table 1. The fixed thresholds in the first and the fourth rules leads to the limitation that these rules are valid to only one particular resolution. We do not impose the relative size to RBC as the area threshold, because the sizes of heterophil vary among avian species. The rules imposed here are for the slide taken at the scale of around 7-8 pixels per micron. On constructing the fourth rule, we assume that there are at most two heterophils clustered together. Our assumption is based on the fact that the size of the heterophil can vary and there is only a few WBC per slide image. It is very unlikely that there are three or more heterophils clustered together.

Table 1. Statistics of heterophils in Type-1 slide and its detection rules.

Statistics	Cell size (pixel)	%Cytoplasm	%Nucleus
Maximum	13,986	91	73
Minimum	3,708	56	21
Decision range (counted as 1 cell)	3,500 – 8,000	50 – 100	15 - 80
Decision range (counted as 2 cells)	> 8,000	50 - 100	15 - 80

CHAPTER 4 - EXPERIMENTS AND RESULTS

4.1. EXPERIMENT SETTING

The proposed iterative thresholding method was tested with different types of chicken blood slides to evaluate both performance and flexibility. The evaluation metric for automatic counting is the percent average error between automatic and manual counting. Less than 5% error is clinically acceptable.

All blood samples were taken from healthy chickens (*Gallus gallus domesticus*) at Faculty of Veterinary Technology, Kasetsart University, Bangkok, Thailand. The method is implemented in MATLAB R2019a on a Lenovo G480 notebook with following specification: CPU Intel® Core™ i5-3230M, RAM 4.00 GB, MS Windows 10 64-bit.

4.2. RBC COUNTING

The objective of this experiment is to verify whether the proposed method is applicable to various staining techniques. Slides with five different appearances of RBC are used as the test images. Except Type-4 slide, each type consists of 10 samples. For Type-4 slide, there are 5 samples. Figure 13 shows the sample slide of each type. The parameters were set by the experiment described in Methodology chapter. An image is divided into five regions according to the experiment on 30 Type-1 slides and the value of k is set to 1 according to the experiment on the Type-1 and Type-2 slides. The only parameter required from the user is which threshold among the four possible thresholds (in Otsu's multiple thresholding) should be used for nucleus detection. In this experiment, except for Type-5 slide, the second lowest threshold was used to detect the nuclei. The third lowest threshold was use for the Type-5 slide.

In Mizutama [18], five parameters need to be carefully selected for accurate counting. It is not designed to cope with different slide appearance. So, it was not chosen as the standard method in this experiment. The counting by CellProfiler [16] also failed to produce the good result, since nuclei are not correctly detected by its robust

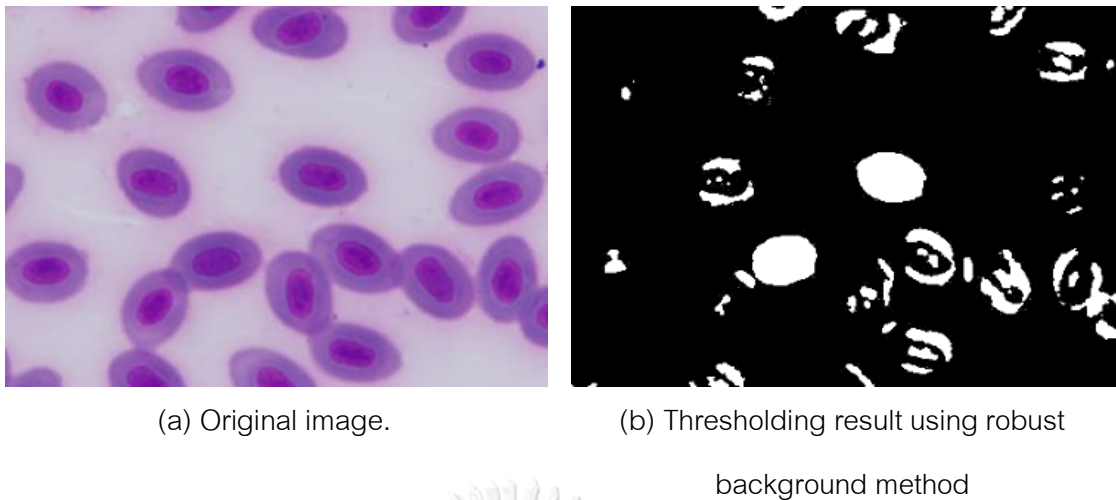


Figure 18. The result of robust background thresholding method in CellProfiler background method as shown in Figure 18. Double thresholding method [17] is simple and can be easily adapted to different staining technique. However, it is simply a single thresholding method without any additional post processing algorithm and it has a scaling parameter “sensitivity” which must be set via experiment. We tried using double thresholding without the scaling parameter in place of Otsu’s multiple thresholding method as the initial threshold value. Though its accuracy was comparable to our method in most case, its accuracy was greatly deteriorated in Type-3 slide.

Table 2 shows the %error of RBC counts. Except for Type-3 slide, our proposed method achieved the clinically acceptable precision (less than 5% error). The cause of accuracy drop in Type-2 slide is that the intensity of the nuclei and the one of the cytoplasm are close, so the extraction of possible nucleus region contains more error. The cause of error in Type-4 slide is due to the existence of the white blood cells whose intensity is close to RBC nuclei.

The large accuracy drop in Type-3 slide is due to the existence of cell’s boundary which is darker than the nucleus. In the proposed method, the nucleus is extracted under the assumption that it is the darkest region in the cell. Therefore, the method fails to differentiate between the boundary and nucleus leading to the counting failure.

Table 2. Performance of automatic RBC count for different types of slide.

RBC Count	Type of Slide					Method / Initial Threshold Value for Iteration
	Type-1	Type-2	Type-3	Type-4	Type-5	
%Average Error	1.408	3.540	8.591	4.797	2.153	Otsu's Multiple Thresholding
	1.369	3.629	16.747	4.948	3.198	Double Thresholding [17]
	1.021	4.247	7.485	2.958	2.906	Otsu's Multiple Thresholding with Post-processing
	1.080	4.216	13.762	4.038	5.095	Double Thresholding [17] with Post-processing

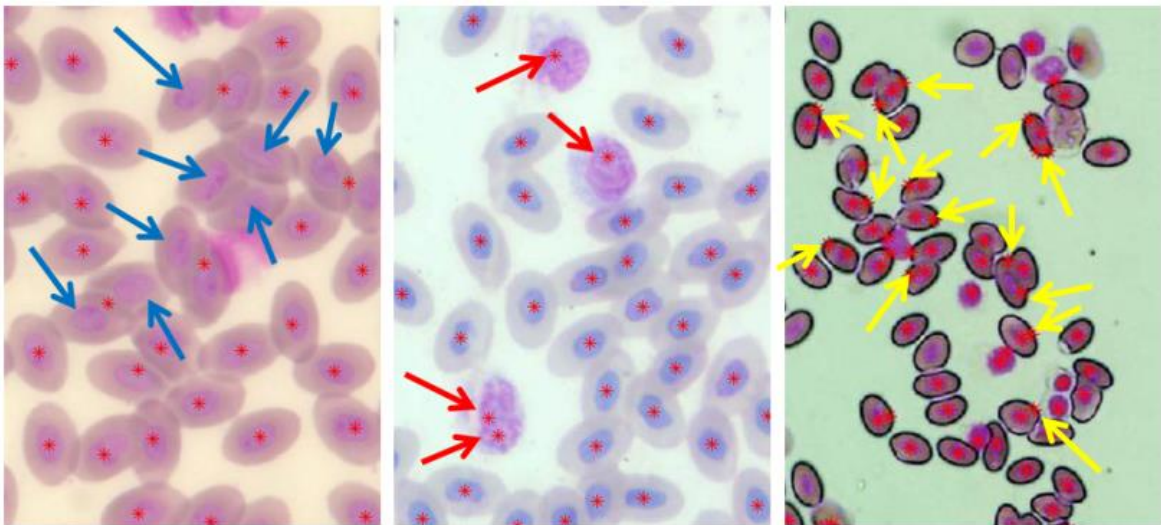
Table 3. Performance of manual RBC count for different types of slide.

RBC Count	Type of Slide					Human Subject
	Type-1	Type-2	Type-3	Type-4	Type-5	
%Average Error	0.308	0.934	1.069	0.371	0.303	Number 1
	0.188	1.454	0.588	0.055	0.169	Number 2
	0.119	0.519	0.480	0.316	0.133	Number 3

In summary, the three major causes of error in our proposed method are as follows.

1. Nuclei are blended into the cytoplasm and not clearly visible (Figure 19(a)).
2. The (grayscale) intensity of WBCs and the one of the nuclei are close (Figure 19(b)).
3. The boundary of RBCs is darker than nucleus (Figure 19(c)).

The gold standard in Table 3 is the manual counting from one human subject. Since manual counting produces different numbers of RBC, we conduct an additional experiment. Three human subjects are requested to count the number of RBC and the average of the three counting is used as the gold standard. Except Type-4 slides which had 5 samples, there were 6 samples per type. Table 3 shows the average counting error (different from the mean) of the three manual counts. The low counting error among human subject (<1.5%) indicates that we can use only one manual count as a gold standard.



(a) False detection caused by nuclei blending to the cytoplasm (Type-2). (b) False detection cause by WBC (Type-5). (c) False detection cause by edge being darker than the nucleus (Type-3).

Figure 19. Three major causes of incorrect RBC detection (red dots show detected nuclei and color arrows show false detection).

4.3. RBC COUNTING WITH POST-PROCESSING

The results after post-processing (DBSCAN) in Table 2 show that the algorithm can reduce error for Type-1, 3, and 4 slides. The efficiency of post-processing varies among different type, because the algorithm is developed and the parameters are set mainly for Type-1 slide. The post-processing efficiency is mainly depended on the quality of segmented nuclei and the surrounding cytoplasm since they are the information used to create data for clustering in DBSCAN. Figure 20 shows example of extracted nuclei of each type of slide. We can see that the nuclei extracted in Type-1, and 5 slides are the most accurate. However, the extracted cytoplasm of the Type-5 slide is not complete. Therefore, the postprocessing is not effective in the Type-5 slides. The nuclei extracted in the Type-4 slide are not very accurate but still consistent. The cytoplasm is also completely extracted after dilated. Therefore, the post-processing of the Type-4 slide is

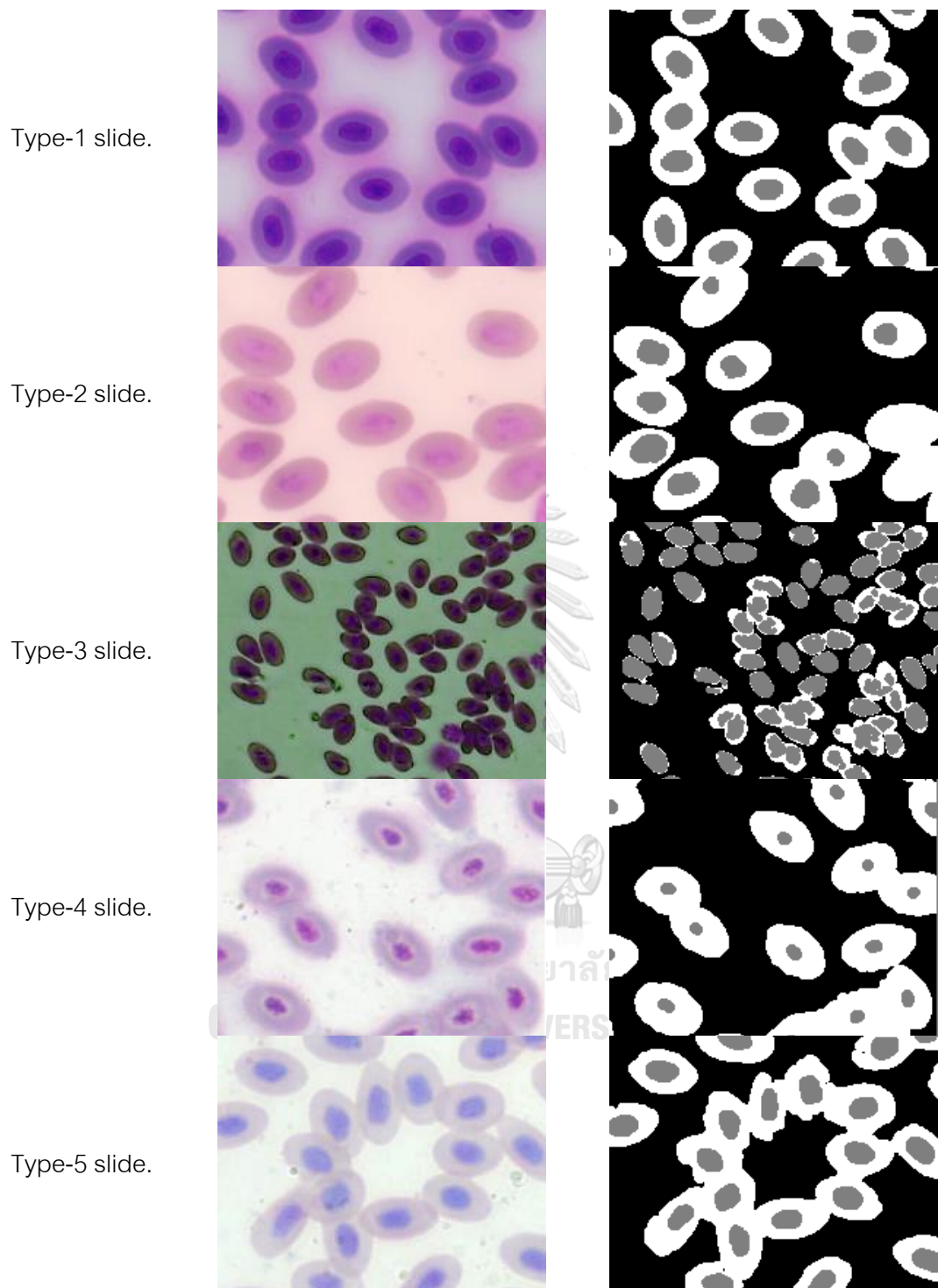


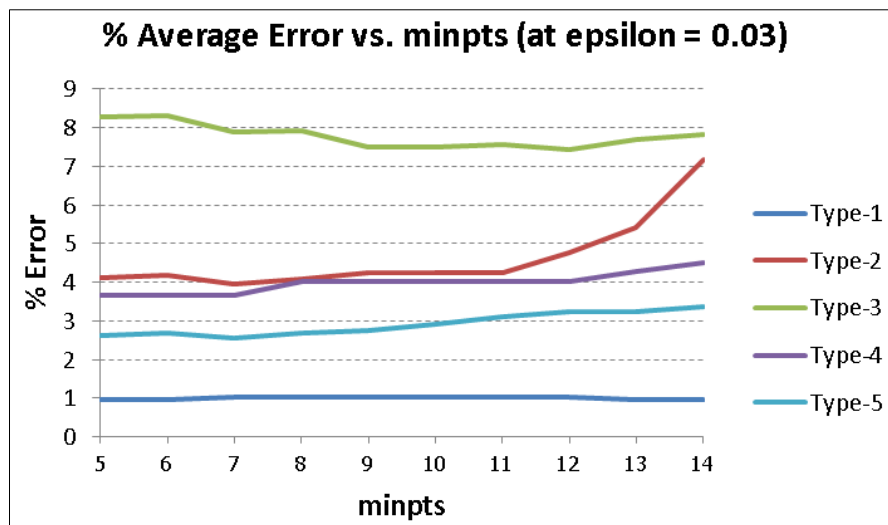
Figure 20. Example of extracted nuclei (shown in gray) in each type of slide (right) and their original image (left).

still effective. The nuclei extracted in Type-2, and 3 slides are not accurate and inconsistent.

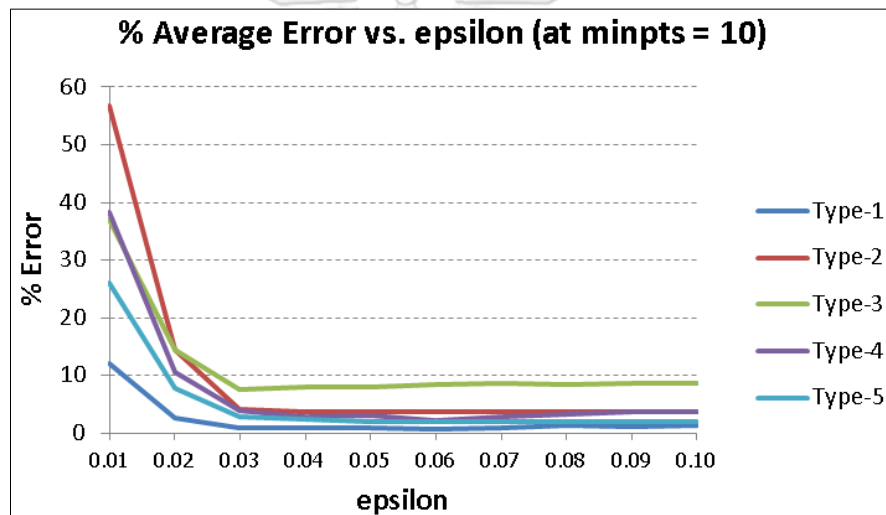
We additionally run an experiment with different values for minpts and epsilon in the following range, respectively: 5 - 14, and 0.01 - 0.10. Figure 21(a) and (b) shows the effect of the minpts and epsilon to the counting error, respectively. Besides Type-2 slide, the segmentation accuracy of DBSCAN is robust to the setting of minpts. Low epsilon leads to higher error; however, when the epsilon is 0.03 or larger, the effect of epsilon is also low. Nevertheless, the graphs show that there exist values that give slightly better result than the parameters selected for Type-1 slide (minpts = 10, epsilon = 0.03).

Table 4 shows the error when the minpts and epsilon were set to the best value as compared to the counting without DBSCAN and the counting with DBSCAN set to the parameter for Type-1 slide. It can be seen that the errors of Type-1, 4, and 5 can be further reduced if better parameters for each type are used. The error of Type-2 slide is still worse than the original value, because the extracted nuclei, which are the input of DBSCAN, are inaccurate and inconsistent. Though, the error of Type-3 slide was decreased, the value (7.419%) was still not clinically acceptable. The output from noise filtering in DBSCAN is either equal to or lowers than the original value, hence, the additive error caused by excessive edge of Type-3 is evened out.

From the experiment, we can conclude that DBSCAN can be used to reasonably reduce error caused by non-RBC false detection (such as shown in Figure 19(b).) as long as the RBC nuclei are accurately extracted, or at least, consistent and the extracted cytoplasm is complete.



(a) Average Error vs. minpts (at epsilon = 0.03)



(b) Average Error vs. epsilon (at minpts = 10)

Figure 21. Effect of DBSCAN's parameters

Table 4. Performance of RBC count with different DBSCAN parameters.

RBC Count	Type of Slide					DBSCAN setting
	Type-1	Type-2	Type-3	Type-4	Type-5	
%Average Error	1.408	3.540	8.591	4.797	2.153	Without DBSCAN
	1.021	4.247	7.485	2.958	2.906	Using parameters selected for Type-1 slide (Figure 15.)
	0.776	3.621	7.419	2.281	1.881	Using optimal parameters for each type of slide

4.4. HETEROPHIL COUNTING

The result of heterophil counting for Type-1 slide is shown in Table 5. Note that the error here is computed differently than the one of RBC. Due to the low number of heterophil (roughly only one cell per slide), the error is calculated by combining counts from 30 slides instead. The proposed rule-based method gives the counting error of 8.8%.

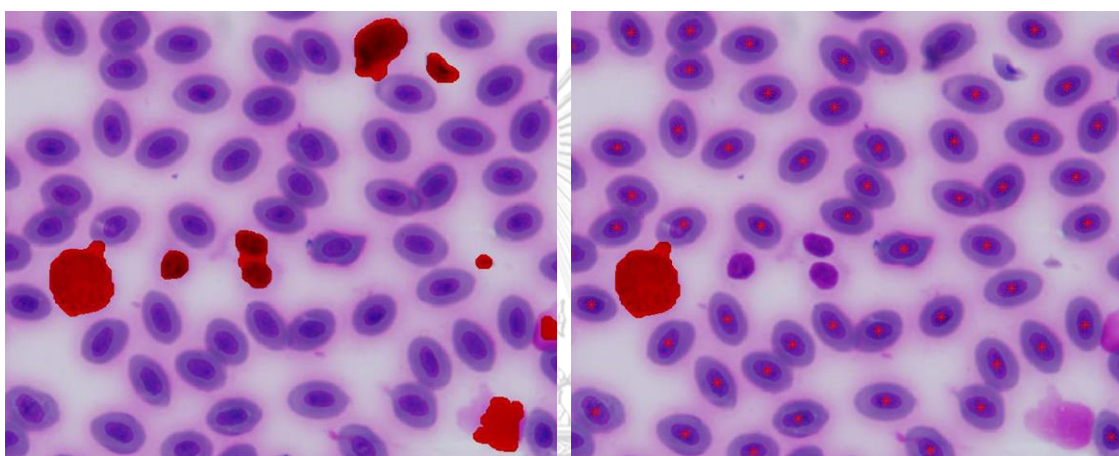
The 8 falsely detected objects are 2 lymphocytes, and 6 miscellaneous objects, such as color stains, shredded cells, etc. The false detected objects have statistics of its intensity similar to heterophil. The method fails to differentiate lymphocyte from heterophil, because our rules are created from the samples having only 2 lymphocytes out of 57 WBCs. It is possible that the rule cannot accurately differentiate WBC type because there are barely any other WBC types existing in our sample; thus, is the limitation of our method. However, we should not ignore that the method successfully filters out many other non-WBCs objects. Figure 22 shows an example of how the method can remove many other objects.

The cause for miss detection is that non-RBCs (in this case, the nucleus of a heterophil) are incorrectly detected as RBCs. The partial region of a WBC is removed, so its appearance does not conform to our rules. If the nucleus is not removed, the heterophil will be correctly detected. As shown in Figure 23, when the nucleus of the heterophil (the red dot in Figure 23(a)) was not removed, the heterophil was correctly detected (the red area in Figure 23(b)).

Unlike RBC, the manual counting for heterophil is fairly simple because counting a couple of WBC is much easier than hundreds of RBC, so there is no need to explore the counting result from multiple subjects.

Table 5. Performance of heterophil count for Type-1 slide.

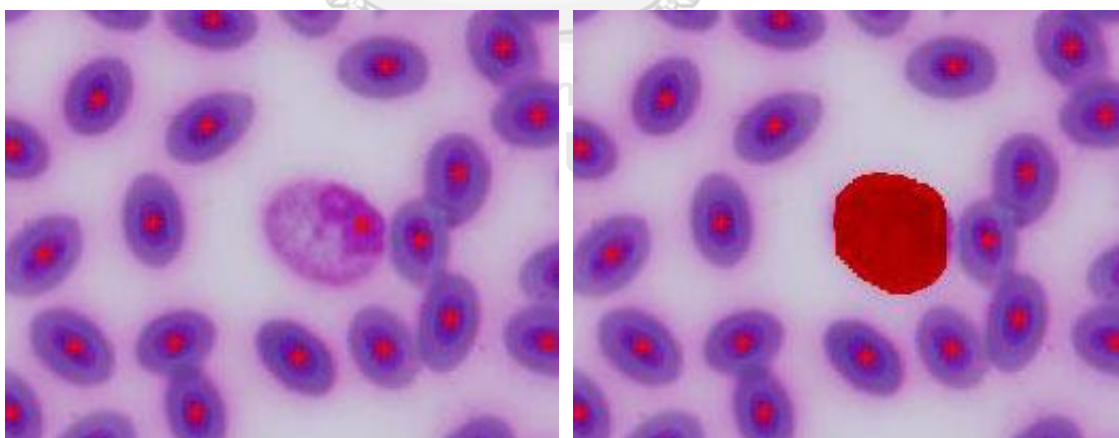
	Heterophil Count	Note
Ground truth	57	-
Proposed method	62	Counting error = 8.772%
Correct detection	54	-
False detection	8	2 are lymphocytes, and 6 are other objects
Miss detection	3	Part of heterophils are considered as RBC in previous steps



(a) Possible WBC regions depicted in red.

(b) Successfully filtered WBC.

Figure 22. Successfully removal of non-WBCs.



(a) Incorrect detection where heterophil is detected as RBC instead (red dot).

(b) Correctly detected heterophil (red area) if the nucleus of the heterophil in (a) is not removed.

Figure 23. Heterophil detection if non-RBCs are correctly removed.

CHAPTER 5 - CONCLUSION

In this research, we propose iterative thresholding method to flexibly count avian RBC and a simple edge detection rule-based method to count heterophil. The results for RBC counting show that 4 out of 5 types of slide are in 5% clinical acceptable range. The post-processing method using DBSCAN can be used to reduce error caused by non-RBCs. The efficiency of DBSCAN is reduced if the color of a RBC's nucleus is closed to the one of cytoplasm or the RBC has dark boundary. We believed that the post-processing by DBSCAN can be more robust to different staining, if the data are processed before we apply DBSCAN. This will be part of our future works.

Heterophil counting error from the proposed rule-based detection method is 8.8% but it can be improved if the rules are better and the post-processing part can filter out non-RBCs more effectively. The method is shown to successfully filter out various non-WBCs. More improvement and insight on heterophil and other type of avian WBC should be possible if there are more available samples.

Because of the similar appearance of blood cells, our proposed method can be easily adapted to analyze the blood of other avian species. It can be used for the health checkup of chicken in broiler industry as well as wild birds for conservation purpose.

REFERENCES

1. Chuasuwan, C. *FROZEN & PROCESSED CHICKEN INDUSTRY*. 2018 [cited 2020 6 Feb]; Available from: https://www.krungsri.com/bank/getmedia/8a42b50e-493d-42fc-8e5e-20dff84a44c9/IO_Chicken_181018_EN_EX.aspx.
2. *Avian and Reptile Estimated White Blood Cell Count*. 2018 [cited 2020 6 Feb]; Available from: <https://www.vet.cornell.edu/animal-health-diagnostic-center/veterinary-support/disease-information/avian-reptile-white-blood-cell-count>.
3. Sahastrabuddhe, A.P., *Counting of RBC and WBC using Image Processing: A Review*. International Journal of Research in Engineering Technology, 2016. **05**: p. 356-360.
4. Maitra, M., R. Gupta, and M. Mukherjee, *Detection and Counting of Red Blood Cells in Blood Cell Images using Hough Transform*. International Journal of Computer Applications, 2012. **53**: p. 13-17.
5. Mazalan, S.M., N.H. Mahmood, and M.A.A. Razak. *Automated Red Blood Cells Counting in Peripheral Blood Smear Image Using Circular Hough Transform*. in *2013 1st International Conference on Artificial Intelligence, Modelling and Simulation*. 2013.
6. Tangsuksant, W., et al. *Development algorithm to count blood cells in urine sediment using ANN and Hough Transform*. in *The 6th 2013 Biomedical Engineering International Conference*. 2013.
7. Cruz, J.C.D., et al. *Microscopic Image Analysis and Counting of Red Blood Cells and White Blood Cells in a Urine Sample*. in *Proceedings of the 2019 9th International Conference on Biomedical Engineering and Technology (ICBET' 19)*. 2019.
8. Davies, E.R., *Finding ellipses using the generalised Hough transform*. Pattern Recognition Letters, 1989. **9**(2): p. 87-96.
9. Yonghong, X. and J. Qiang. *A new efficient ellipse detection method*. in *Object recognition supported by user interaction for service robots*. 2002.

10. Chia, A.Y.S., et al. *Ellipse Detection with Hough Transform in One Dimensional Parametric Space*. in *2007 IEEE International Conference on Image Processing*. 2007.
11. Liu, Z., et al., *Segmentation of White Blood Cells through Nucleus Mark Watershed Operations and Mean Shift Clustering*. *Sensors* (Basel, Switzerland), 2015. 15: p. 22561-86.
12. Tareef, A., et al. *Automatic nuclei and cytoplasm segmentation of leukocytes with color and texture-based image enhancement*. in *2016 IEEE 13th International Symposium on Biomedical Imaging (ISBI)*. 2016.
13. Ahasan, R., A.U. Ratul, and A.S.M. Bakibillah. *White blood cells nucleus segmentation from microscopic images of strained peripheral blood film during leukemia and normal condition*. in *2016 5th International Conference on Informatics, Electronics and Vision (ICIEV)*. 2016.
14. Clark, P., W. Boardman, and S.R. Raidal, *Atlas of clinical avian hematology*. 2009, Oxford Ames, Iowa: Wiley-Blackwell. 200.
15. Autaiem, T., et al. *Automatic Counting for Canine Red Blood Cell based on Two-stage Circular Hough Transform*. in *2019 12th Biomedical Engineering International Conference (BMEiCON)*. 2019.
16. Beaufrere, H., M. Ammersbach, and T.N. Tully, Jr., *Complete blood cell count in psittaciformes by using high-throughput image cytometry: a pilot study*. *J Avian Med Surg*, 2013. 27(3): p. 211-7.
17. Meechart, K., S. Auethavekiat, and V. Sa-ing. *An Automatic Detection for Avian Blood Cell based on Adaptive Thresholding Algorithm*. in *2019 12th Biomedical Engineering International Conference (BMEiCON)*. 2019.
18. Ochoa, D., T. Redondo, and G. Moreno-Rueda, *Mizutama: A Quick, Easy, and Accurate Method for Counting Erythrocytes*. *Physiol Biochem Zool*, 2019. 92(2): p. 206-210.
19. Otsu, N., *A Threshold Selection Method from Gray-Level Histograms*. *IEEE Transactions on Systems, Man, and Cybernetics*, 1979. 9(1): p. 62-66.

20. Liu, Y., et al., *Segmentation of White Blood Cells Image Using Adaptive Location and Iteration*. IEEE Journal of Biomedical and Health Informatics, 2017. 21(6): p. 1644-1655.
21. Ram, A., et al., *A Density Based Algorithm for Discovering Density Varied Clusters in Large Spatial Databases*. International Journal of Computer Applications, 2010. 3.
22. *Density-based spatial clustering of applications with noise (DBSCAN) - MATLAB dbscan*. 2019 [cited 2020 6 May]; Available from: <https://www.mathworks.com/help/stats/dbscan.html>.
23. Gonzalez, R.C. and R.E. Woods, *Digital Image Processing*. 3rd ed. 2008, Upper Saddle River, N.J.: Prentice Hall. xxii, 954 p.





จุฬาลงกรณ์มหาวิทยาลัย
CHULALONGKORN UNIVERSITY

VITA

NAME Tanapat Autaiem

DATE OF BIRTH 20 October 1995

PLACE OF BIRTH Bangkok, Thailand

INSTITUTIONS ATTENDED Bachelor of Engineering

HOME ADDRESS 112/25 Moo.3, Bangkruai-Sainoi Road, Tambon Wat Chalo,
Amphoe Bangkruai, Nonthaburi, 11130

PUBLICATION T. Autaiem, S. Auethavekiat, V. Sa-ing, K. Nakgoi, N.
Prasertsincharoen and P. Arreesnsom, "A Novel Iterative
Method for Automatic Avian Red Blood Cell Counting," 2019
12th Biomedical Engineering International Conference
(BMEiCON), Ubon Ratchathani, Thailand, 2019, pp. 1-5, doi:
10.1109/BMEiCON47515.2019.8990325.